Laser and Particle Beams (2004), *22*, 373–379. Printed in the USA.

DOI: 10.1017/S0263034604223230

Bright, point X-ray source based on a commercial portable 40 ps Nd:YAG laser system

ANATOLY FAENOV,[1] TATIANA PIKUZ,[1] ALEXANDER MAGUNOV[1,2] DIMITRI BATANI,[3] GIANNI LUCCHINI,[3] FEDERICO CANOVA,[3] AND MORENO PISELLI[3]

[1]Multicharged Ions Spectra Data Center (MISDC) of National Research Institute for Physical-Technical and Radiotechnical Measurements, Moscow, Russia
[2]A.M. Prokhorov General Physics Institute of RAS, Moscow, Russia
[3]Dipartimento di Fisica "G.Occhialini", Università di Milano Bicocca, Piazza della Scienza 3, 20126 Milano, Italy

(RECEIVED 1 November 2003; ACCEPTED 28 May 2004)

Abstract

We present some experimental results on X-ray spectra obtained from plasmas produced using a compact Nd:YAG laser system. The beam was focused on different targets (Cu, Al, Ge,…) and both high resolution and low resolution X-ray spectra were recorded.

Keywords: ps laser; X-ray plasma sources; X-ray spectroscopy

1. INTRODUCTION

Laser-plasma sources are very powerful laboratory-scale X-ray devices where wavelength tunability is feasible because of the comparatively free choice of target material, laser wavelength, and intensity. They have already been successfully applied for radiobiology (Turcu *et al.*, 1994*a*; Masini *et al.*, 1999; Milani *et al.*, 1999; Bortolotto *et al.*, 2000), X-ray microscopy (Batani *et al.*, 2000, 2002; Desai *et al.* 2003; Poletti *et al.*, 2004), micro-lithography (Bijkerk *et al.*, 1992; Turcu *et al.*, 1994*b*). For all these applications the knowledge of X-ray spectra is very important, either directly or because energy deposition and radiation dose are strongly energy dependent.

For instance in micro-lithography ~1-keV X-ray photons are required to achieve efficient radiation transfer through the X-ray mask membrane and sufficient energy deposition onto the resist coated Si wafer.

In radiobiology, laser-plasma X-ray sources were used to irradiate biological specimens: V-79 Chinese hamster cells (Turcu *et al.*, 1994*a*), and study DNA damage, DNA repair and repair inhibition, or Saccharomices Cerevisiae yeast cells (Masini *et al.*, 1999; Milani *et al.*, 1999) and study metabolic damages. In the first case, X-rays at $h\nu \approx 1.2$ keV were produced using L-shell emission from Cu targets, which could guaranty penetration of X-rays to the cell nucleus, so that absorbed dose was really related to DNA damage. In the second case, it was essential to produce low energy X-ray photons, which would mainly deposit the dose at the cell wall, in order to produce damages at the metabolic level without touching the cell nucleus.

Finally in X-ray microscopy, the spectrum is important because only X-rays in the "water window" (between 22 and 44 Å) will contribute to the formation of a clean image, being absorbed by biological material but not by water. The presence of other X-ray lines will diminish the image contrast dramatically.

Besides all this, the study of X-ray spectra from plasmas is very important in itself and it is a well developed field in physics. Indeed on one side, X-ray spectra are very important for atomic physics because by recording X-ray emission lines, it is possible to access the energy levels in atoms and in multi-charged ions (Rosmej *et al.*, 1997; Stepanov *et al.*, 1997; Vergunova *et al.*, 1997; Biemont *et al.*, 2000). On the other side, X-ray spectroscopy is a key technique in plasma diagnostics (Koenig *et al.*, 1997; Magunov *et al.*, 1998; Batani *et al.*, 1999) since from measurements of X-ray spectra we can calculate the plasma parameters: electron density, electron temperature, ion charges, and even deduce important information on plasma opacities and on the exact shape of the electron distribution function (including the presence of fast electrons)

A key problem for applications and for X-ray spectroscopy, would be the development of very compact X-ray sources which would be cheap (and be reproduced in many

Address correspondence and reprint requests to: Anatoly Faenov, MISDC, National Research Institute for Physical-Technical and Radiotechnical Measurements, Moscow 141570, Russia. E-mail: faenov@yahoo.com

laboratories and universities) and even transportable. In this context, we have used a very compact laser system and we have used it for X-ray spectroscopic studies. We have recorder X-ray spectra from various materials (Cu, Al, Ge, Si, SiO2, Si-gel) using both flat crystal Bragg minispectrometers (low resolution, wide spectral range) and curved crystal spectrometers, giving a very high resolution in a small spectral range.

The characteristics of the laser sources (self filtering unstable resonator cavity) implied a very good beam quality so that a very small focal spot could be obtained, implying a very good spectral resolution in the collected experimental spectra.

2. EXPERIMENTAL SET-UP

2.1. Laser system

The laser used for the experiments is situated at the Department of Physics of the University of Milano-Bicocca (see Fig. 1). It is an active-passive mode-locked Nd:YAG system (SYL P2, produced by Quanta System Srl, Solbiate, Italy), and consists of a laser oscillator, an amplifier, and a nonlinear crystal (KD^*P) for second harmonic conversion. It can operate with a repetition frequency from 0.5 to 10Hz or in single shot.

The oscillator is based on a Self Filtering Unstable Resonator (SFUR) cavity, which gives the advantages of a large mode diameter and a high beam quality. This assures a high energy per pulse and a high focusability, which are essential in order to reach high intensities (of the order of 10^{14} W/cm^2) and allow efficient X-ray generation. Also, the very small size of the focal spot (that is, of the X-ray source) is an advantage in getting a very high spectral resolution. A pulse duration of about 40 ps is achieved by using a saturable absorber dye (Exciton Q-switch 1 MW 763.33) and an Acousto-Optic standing-wave Modulator. The laser pulse is extracted from the oscillator by cavity dumping through an intracavity Pockels' cell.

The amplifier rod has a diameter of 9.5 mm and a length of 110 mm. A good filling factor is assured by enlarging the oscillator beam with a telescope while keeping a moderate beam clipping in order to prevent the generation of diffraction rings. The second harmonic at 532 nm and the first harmonic at 1,064 nm are separated by two dichroic mirrors and are available at two different laser outputs.

Pulse duration was measured with a second-harmonic scanning autocorrelator to be 40 ± 2 ps, in agreement with constructor's data. The autocorrelator, based on an interferometric scheme (with a movable mirror with a possible displacement of several cm), used a KDP crystal. A typical autocorrelator trace is shown in Figure 2. From the FWHM Δx of such trace we can calculate the pulse duration Δt by recalling that every displacement of the movable mirror implies a double path for the optical ray, and that a further $\sqrt{2}$ factor accounts for the different FWHM of the autocorrelation trace and of the laser pulse intensity.

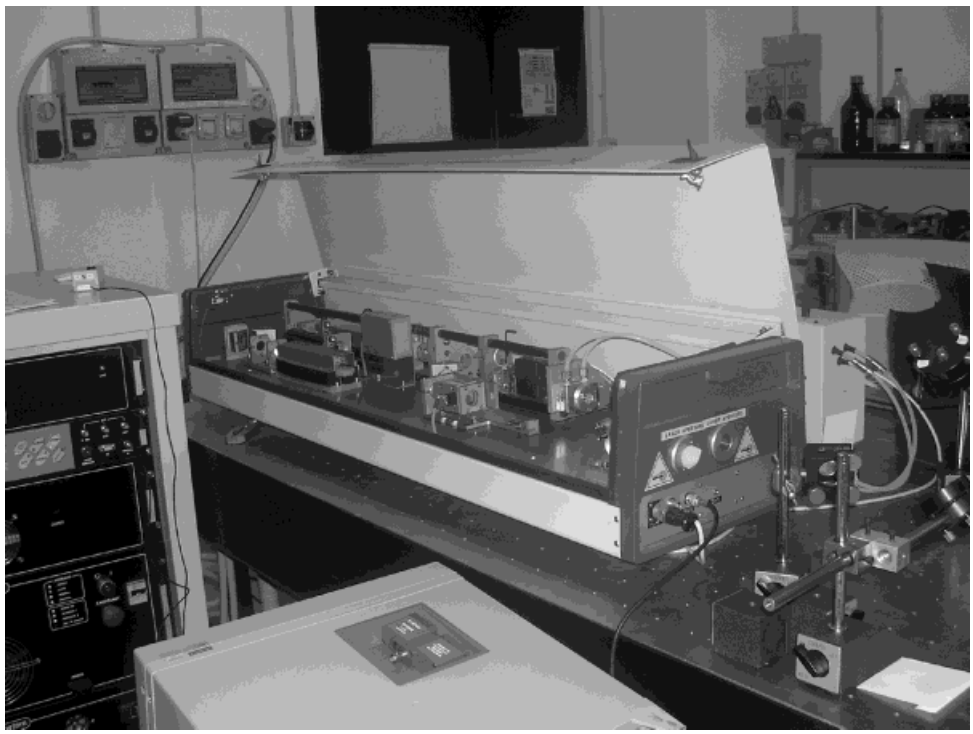

Fig. 1. Laser system installed at the Department of Physics of the University of Milano-Bicocca. It is a very compact (laser head: $325 \times 225 \times 1280$ mm, 40 kg) active-passive mode-locked Nd:YAG system (SYL P2, produced by Quanta System Srl, Italy).

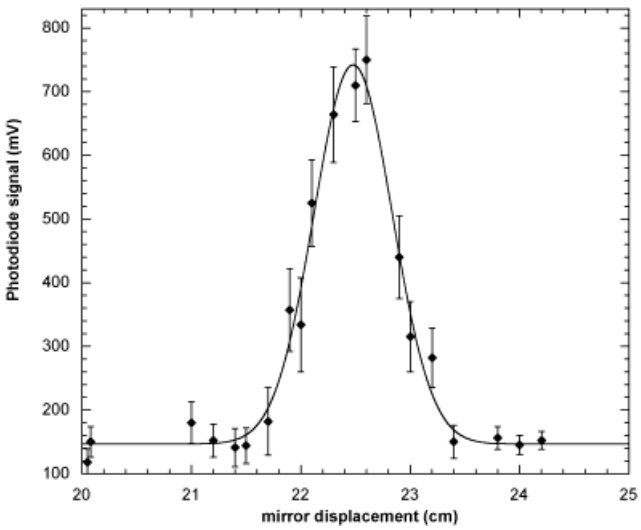

Fig. 2. Autocorrelation trace, obtained with a scanning second-harmonic autocorrelator, fitted with a gaussian curve giving a pulse duration of 40 ± 2 ps.

The beam was focused onto the target with an f = 5 cm lens, obtaining a focal spot radius of about ≥ 10 μm. This was directly measured using a CCD, which was moved along the beam path in order to measure the different beam radii for different relative position of the CCD and the lens. Figure 3 shows our experimental data and the interpolation with the hyperbole

$$a(z) = \sqrt{a_0^2 + \left(\frac{D}{2f}(z-f)\right)^2},$$

where D is the initial diameter of the beam (measured on the lens or at the output of the amplifier), f is the focal length, and a_0 is the focal spot diameter.

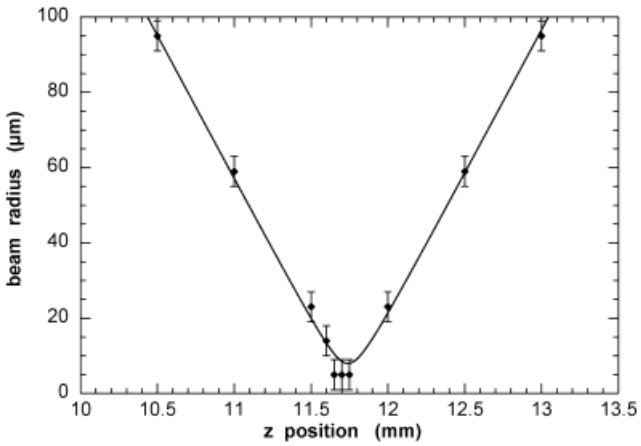

Fig. 3. Variation of beam radius (corresponding to FWHM) and interpolation with a hyperbole giving a focal spot radius of about 10 μm. This was obtained with an f = 5 cm lens and measured with a 16-bit CCD with Kodak 0400 chip, with 9 μm pixels.

The laser pulse energy was measured shot-by-shot by a calorimeter, which was collecting the reflection from the prismatic entrance window of the interaction chamber (this was absolutely calibrated, during the preparation of the experiment, with a calorimeter placed after the focusing lens). The energy of the pulse was typically 20 mJ from which we could calculate a laser intensity on target of a few times 10^{14} W/cm^2, at the second harmonic.

Energy in first harmonic was larger, however X-ray emission was much fainter due to a prepulse problem. Indeed at each round trip in the laser cavity, a small part of the laser pulse comes out of the cavity, due to the low extinction coefficient of the Pockel's cells and polarizers, and is afterward amplified in the amplifier rod. This creates a train of 5–6 pulses before the main laser pulse (the one extracted by cavity dumping) with a typical contrast ration of a few percent and a total duration of 50–60 ns (the round trip time being 10 ns). This train strongly affected the production of X-ray by creating a diluted preplasma in front on the main target, so that the interaction of the main pulse took place with such preplasma. In the second harmonic, due to the non-linear nature of SHG, the problem was greatly reduced and efficient X-ray generation was observed. In this first preliminary paper we will only deal with results obtained at 2ω.

The target was placed in a vacuum chamber and the beam was sent to the chamber by two high reflecting mirrors (45°, 2ω). The interaction chamber is a small cylindrical chamber (height = 35 cm, diameter = 40 cm, see Fig. 4), which in a short time can be evacuated by a rotative vacuum pump. The target was a flat thick foil placed perpendicularly to the beam, which could be moved along the x and y direction by external motions. The lens could be remotely moved along the z-axis (optical axis) with an external digitally controlled micrometric motion. The focusing of the laser beam was checked by measuring the X-ray signal with two silicon PIN diodes filtered with different foil thickness so to look at softer and harder X-rays. The FWHM of the curve showing X-ray PIN diode signal vs. z, was comparable to the focal depth of our lens. The lens was accurately normalized before the beginning of X-ray exposure.

2.2. X-ray spectrometers

The X-rays emitted by the plasma were recorded by using both flat crystal Bragg minispectrometers (low resolution, large spectral range) and two spectrographs with spherically bent quartz crystal (high spectral resolution).

First, we used two flat-crystal Bragg minispectrometer equipped with Beryl and RbAP crystal (respectively, 2D = 15.95 and 26.121 Å). These were filtered with thin Al foils to stop visible and XUV radiation. X-ray spectra were recorded on Kodak DEF X-ray film (Rockett *et al.*, 1985) following exposure to about 100 laser shots. These flat crystal spectrometers offer the advantage of allowing a wide spectral range to be recorded, which can be useful for diagnostics purposes. However, the spectral resolution is

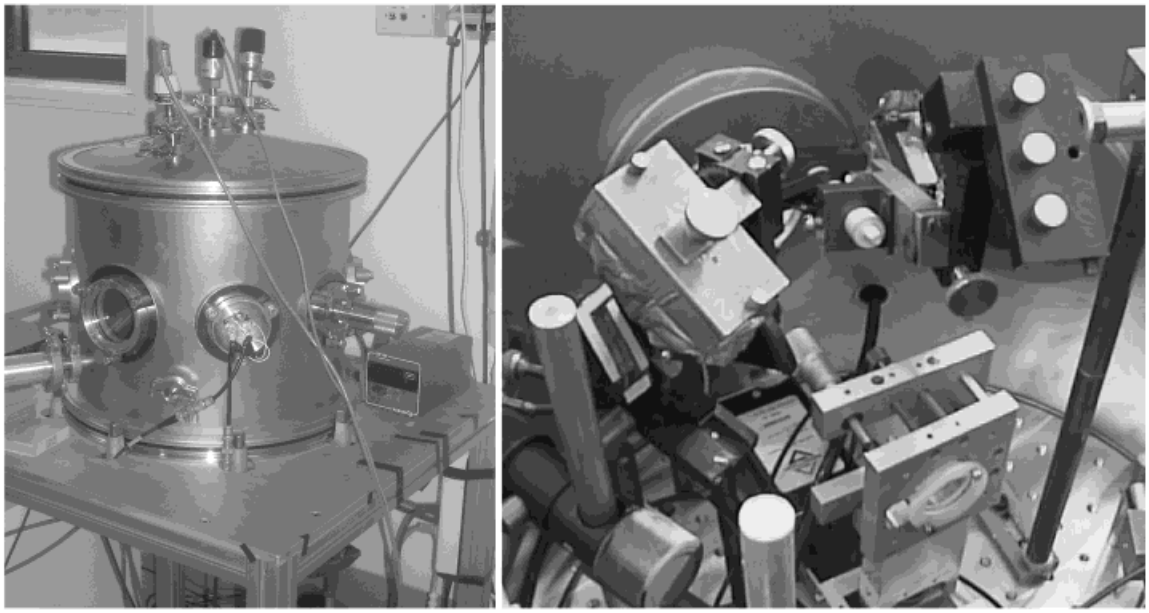

Fig. 4. (a) Vacuum and interaction chamber (height = 35 cm, diameter = 40 cm) produced by RIAL Vacuum, Italy, equipped with Pirani vacuum gauge and 8 BK7 glass windows. up and bottom flanges DN 400 ISO LF. The upper flange is curved in order to withstand atmospheric pressure with a thinner wall. (b) The interior of the chamber showing the focusing lens and the two FSSR-1D spectrometers.

not high and is typically limited by source size (in our case however this is not so bad thanks to the small source size) and luminosity is quite low, implying that a large number of laser shots is needed even for recording X-ray spectra from materials such as Cu, which are very efficient emitters in the low X-ray region.

Second, we used curved crystal spectrometers, which have the advantage of high spectral resolution and high luminosity. The configuration used for the spherically bent quartz crystal spectrometers is of the type FSSR-1D (Faenov *et al.*, 1994; Pikuz *et al.*, 1995): in this scheme, see Figure 5, the X-ray detector stays out of the Rowland circle. The radius of curvature of the crystal is R = 10 mm and interatomic distance is 2D = 0.85 nm. The effective spectral resolution obtained in the experiment was better than $\lambda/\Delta\lambda >$ 500. Spatial resolution is around 15 μm and magnification is one to one.

The two spectrometers were centred at different wavelengths, so we could obtain information on a wider spectral region for the same laser conditions. The X-ray spectra were

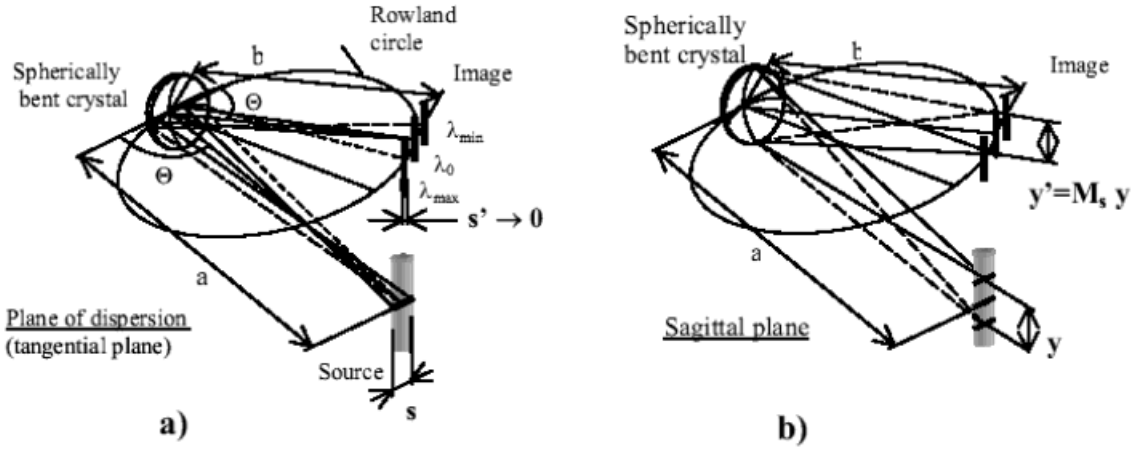

Fig. 5. The FSSR-1D scheme: formation of the spectral resolution in the dispersion (meridian) plane (a); formation of the spatial resolution in the sagittal plane (b).

recorded in the first Bragg reflection order on Kodak DEF or RAR films. On the spectrometer there was a PA filter (2 μm C_3H_6 and 0.4 μm Al) to cut visible and VUV radiation. For some spectra there were also a Be filter to attenuate the soft X-ray radiation in the region from 0.5 to 0.75 nm.

3. RESULTS

3.1. Low resolution spectra

A typical low resolution spectrum of Cu is shown in Figure 6. This was obtained with a flat crystal Bragg minispectrometer equipped with a RbAP crystal on Kodoak DEF film. It shows emission lines from Ne-like (Cu XX), F-like (Cu XXI), and O-like (Cu XXII) ions. Average emission is at at h$\nu \approx 1.2$ keV. Lines have been compared with information available in the literature (Batani *et al.* 1991; Kelly, 1987; Hutcheon *et al.*, 1980; Gordon *et al.*, 1980). The lines reported in Figure 6 are also listed in Table 1.

3.2. High resolution spectra

Spectra of H- and He-like Al and Si and also Ne-like Ge and Yttrium have been measured in the spectra range 5–8 Å using two FSSR-1D spectrometers with spherically bent quartz 10-10 (2D = 8.5 Å) crystals. Spectrometers have been placed at the angles 45 and 70 degrees to the target. From 1 to 130 shots have been necessary to record good spectra on RAR 2492 film. Due to the small size of the laser spot and high resolved power of used spectrometers (theoretical apparatus spectral resolution for such spectral range is in the order of 5,000–10,000), spectral resolution of obtained spectra were $\lambda/\Delta\lambda \geq 500$, and mainly depended on the Doppler and Stark broadening of the spectral lines. Also since the FSSR-1D is imaging in the saggital plane, we could confirm the very small size of the X-ray source.

Figures 7 and 8 show typical spectra in the vicinity of Rydberg ($n = 4,5,6 - n' = 2$) lines of Ne-like Ge XXIII, obtained in 20 laser shots. Intensities of 4-2 transitions of Ne-like Ge was too high, producing overexposed lines on the film, because many laser shots were necessary to obtain a sufficient intensity for the Rydberg lines of Ne-like ions with higher values of *n*.

Figures 7 and 8 also show spectra of Rydberg lines of He-like Al and Lyα of H-like Al. Both spectra have been obtained on the same film with a small space shifting (Al target has been shifted of 0.5 mm in comparison with Ge target). In this way, the very well-known spectral lines of Al

Table 1. *Experimental and tabulated wavelengths of lines observed in the Cu spectrum*

λ exp (Å)	λ tab (Å)	$\Delta\lambda$ (Å)	Ion		Transition
12.820	12.830	0.01	Ne	Cu XX	$2s^22p^6$–$2s^22p^53s$
12.565	12.573	0.008	Ne	Cu XX	$2s^22p^6$–$2s^22p^53s$
12.140	12.140	0	F	Cu XXI	$2s^22p^5$–$2s^22p^43s$
12.025	12.061	0.036	F	Cu XXI	$2s^22p^5$–$2s^22p^43s$
11.921	11.920	0.01	F	Cu XXI	$2s^22p^5$–$2s^22p^43s$
11.829	11.830	0.001	F	Cu XXI	$2s^22p^5$–$2s^22p^43s$
11.760	11.737	−0.023	Ne	Cu XX	$2s^22p^6$–$2s^22p^53d$
11.600	11.597	−0.003	Ne	Cu XX	$2s^22p^6$–$2s^22p^53d$
11.390	11.386	0.004	Ne	Cu XX	$2s^22p^6$–$2s^22p^53d$
11.245	11.229	−0.016	F	Cu XXI	$2s^22p^5$–$2s^22p^43d$
11.126	11.136	0.01	F	Cu XXI	$2s^22p^5$–$2s^22p^43d$
11.072	11.065	0.007	F	Cu XXI	$2s^22p^5$–$2s^22p^43d$
11.020	11.026	−0.006	F	Cu XXI	$2s^22p^5$–$2s^22p^43d$
10.975	10.971	0.004	F	Cu XXI	$2s^22p^5$–$2s^22p^43d$
10.892	10.893	−0.001	F	Cu XXI	$2s^22p^5$–$2s^22p^43d$
10.870	10.863	−0.007	F	Cu XXI	$2s^22p^5$–$2s^22p^43d$
10.822	10.800	0.022	F	Cu XXI	$2s^22p^5$–$2s^22p^43d$
10.660	10.653	−0.007	O	Cu XXII	$2s^22p^4$–$2s^22p^33d$
10. 610	10.597	−0.013	O	Cu XXII	$2s^22p^4$–$2s^22p^33d$
10.562	10.551	0.011	O	Cu XXII	$2s^22p^4$–$2s^22p^33d$
10.508	10.522	−0.014	O	Cu XXII	$2s^22p^4$–$2s^22p^33d$
10.411	10.422	−0.011	O	Cu XXII	$2s^22p^4$–$2s^22p^33d$
10.380	10.392	−0.012	O	Cu XXII	$2s^22p^4$–$2s^22p^33d$
10.323	10.316	0.07	O	Cu XXII	$2s^22p^4$–$2s^22p^33d$
10.285	10.277	0.008	O	Cu XXII	$2s^22p^4$–$2s^22p^33d$

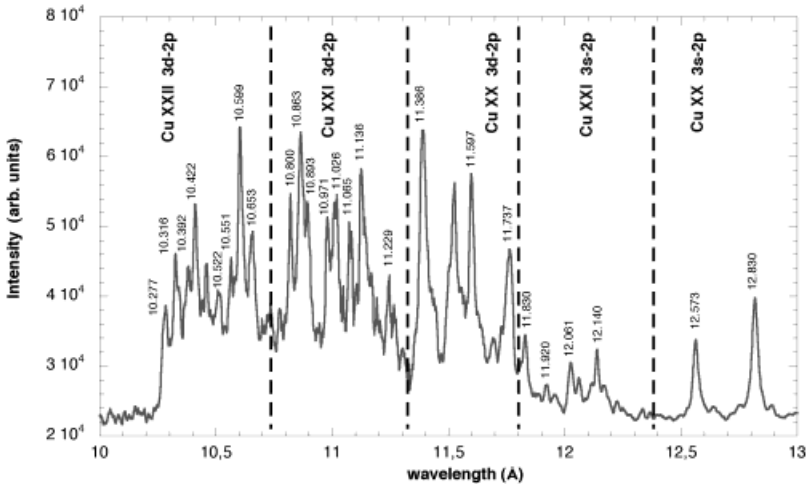

Fig. 6. X-ray spectrum from Cu obtained with a RbAP crystal on kodoak DEF film. It shows emission lines from Ne-like (Cu XX), F-like (Cu XXI), and O-like (Cu XXII) ions.

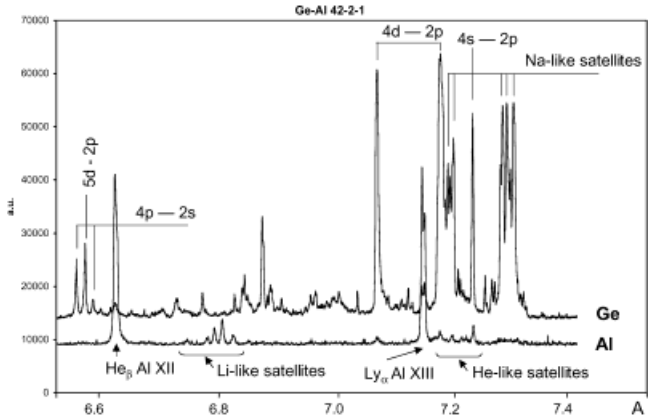

Fig. 7. Typical spectra from one FSSR-1D spectrometer in the spectral range 6.5–7.5 Å. The two Ge and Al spectra were obtained on the same RAR film by slightly moving the target.

could be used as a reference for wavelengths measurements of Ge spectral lines.

Obtained intensities of spectra (small intensities of He-like satellites near the Lyα of H-like Al as compared with resonance line and Li-like satellites near the Heβ line of Al) give the possibility of estimating an electron temperature of the laser-produced plasma of about 500 eV. A relatively high temperature and high brightness in X-ray spectral range of used laser plasma source also follow from the fact that intense spectra of Resonance line of He-like Al could obtained only in 1 laser shot.

More quantitatively, high-resolution X-ray spectra of plasmas produced from aluminium and silicon solid targets were analysed for determining plasma parameters. The relative X-ray intensity in the spectral region 0.52–0.71 nm was obtained from the measured data taking into account the non-linear dependence on the film density, the quartz crystal reflectivity and the filter transmission.

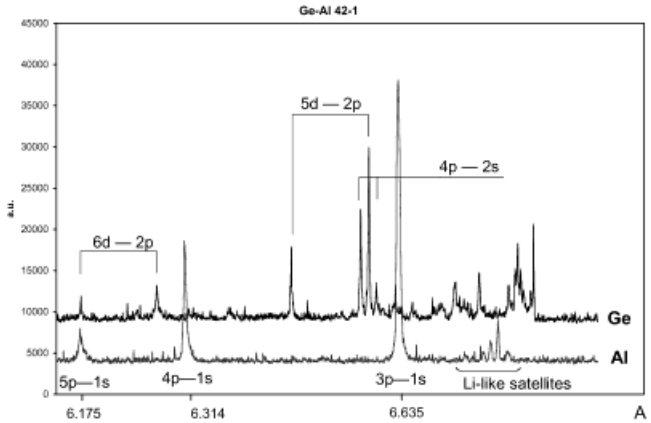

Fig. 8. X-ray spectrum from the other FSSR-1D spectrometer in the spectral range 6.1–6.9 Å in the vicinity of Rydberg ($n = 4,5,6$-$n' = 2$) lines of Ne-like Ge XXIII, obtained in 20 laser shots. Also shown the Heβ and Lyα lines from Al with corresponding satellites.

The shape of the resonance Lyα line of the H-like ion and the 1s2p $^1P_1$–1s^2 $^1S_0$ line of the He-like ion, and the values of their intensities with respect to the intensity of dielectronic satellite lines (corresponding to the X-ray transitions from the autoionizing states of lower charged ions) were compared with model calculations to obtain the electron temperature values.

The intensity ratio for the resonance and intercombination lines 1s2p $^{1,3}P_1$–1s^2 $^1S_0$ of the He-like ion was used to obtain the electron density by fitting kinetic model results to the experimentally observed values. The plasma opacity was taken into account for correct comparison of the experimentally observed resonance line intensity with the calculation for optically thin plasmas.

The analysis gives values of the electron temperature in the range 450–600 eV for different Si plasmas (pure Si, SiO_2 and Si-gel targets) and about 740 eV for Al plasma, at an electron density $(1.3–1.6)\cdot 10^{21}$ cm^{-3}.

These values of plasma parameters can be independently proved or corrected by further more detailed calculations of the line shape and intensities for experimentally observed high–n transitions 1snp $^1P_1$–1s^2 $^1S_0$ (n = 3–5), using the Stark line profile and collisional-radiation kinetic model codes.

4. CONCLUSIONS

We have presented experimental results on X-ray spectra obtained from plasmas produced using a small Nd:YAG laser system. The beam was focused on different targets (Cu, Al, Ge, Si, SiO2, Si-gel) and both high resolution and low resolution X-ray spectra were recorded. The source seems to be very promising thanks to the very good focusability which offers the possibility of measuring X-ray spectra with a very high spectral resolution. Also the quite large pulse energy (more than 100 mJ in the first harmonic) and quite high repetition frequency (up to 10Hz) offers the possibility of recording X-ray spectra from various target materials even with relatively low X-ray emission, by accumulating in a short time several shots on the X-ray film. A more detailed analysis of collected X-ray spectra is presently in progress.

ACKNOWLEDGMENTS

We warmly acknowledge the help of Dr. Marco Tagliaferri, Quanta Systems, for the help in setting up the laser system. The stay of A. Faenov, T. Pikuz, and A. Magunov at the University of Milano Bicocca was supported by a grant of the European Science Foundation (ESF) in the framework of the Scientific Programme FEMTO.

REFERENCES

Batani, D., Turcu, E., Tallents, G. Giulietti, A. & Palladino, L. (1991) L-shell X-ray spectroscopy of laser-produced plasmas in the 1-keV region. In *Excimer Lasers and Applications III* SPIE **1503**, 479–491.

Batani, D., Koenig, M., Benuzzi, A., Boudenne, J.M., Cauchon, G., Hall, T. & Nazarov, W. (1999). X-Ray Diagnostic Applied to the Study of Shock Wave Propagation in Foams. *Review Scientific Instruments* **70**, 1464–1467.

Batani, D., Botto, C., Bortolotto, F., Masini, A., Bernardinello, A., Moret, M., Poletti, G., Cotelli, F., Lora Lamia Donin, C., Piccoli, S., Stead, A., Ford, T., Marranca, A., Eidmann, K., Flora, F., Palladino, L. & Reale, L. (2000). Contact X-ray microscopy using the Asterix laser source. *Physica Medica* **14**, 49.

Batani, D., Botto, C., Bernardinello, A., Moret, M., Cotelli, F., Lora Lamia Donin, C., Stead, A., Ford, T. & Eidmann, K. (2002). The use of high energy laser-plasma sources in soft X-ray contact microscopy. *European Physical Journal D* **21**, 167.

Biemont, E., Magunov, A., Dyakin, V., Faenov, A., Pikuz, T., Skobelev, I., Osterheld, A., Goldstein, W., Flora, F., Di Lazzaro, P., Bollanti, S., Lisi, N., Letardi, T., Reale, A., Palladino, L., Batani, D., Mauri, A., Scafati, A. & Reale, L. (2000). Measurement of the ground state ionisation energy and wavelengths for the 2l-nl′ transitions of Ni XIX (n=4–14) and Ge XXIII (n=7–9). *Journal of Physics B: At. Mol. Opt. Phys.* **33**, 2153–2162.

Bijkerk, F., Louis, E., Van der Wiel, M., Turcu, E., Tallents, G.J. & Batani, D. (1992). Performance optimisation of a high repetition rate KrF laser plasma X-ray source for microlithography. *Journal of X-ray Science and Technology* **3**, 133–151.

Bortolotto, F., Batani, D., Previdi, F., Rebonato, L. & Turcu, E. (2000). Study of a X-ray laser-plasma source for radiobiological experiments, microdosimetry analysis and plasma characterisation. *European Physical Journal D* **11**, 309.

Desai, T., Batani, D., Bernardinello, A., Poletti, G., Orsini, F., Ullschmied, J., Juha, L., Skala, J., Kralikova, B., Krousky, E., Pfeifer, M., Kadlec, Ch., Mocek, T., Präg, A., Renner, O., Cotelli, F., Lora Lamia, C. & Zullini, A. (2003). X-ray Microscopy of living multi-cellular organisms with PALS. *Laser Part. Beams* **21**, 509–514.

Faenov, A.Ya., Pikuz, S.A., Erko, A.I., Bryunetkin, B.A., Dyakin, V.M., Ivanenkov, G.V., Mingaleev, A.R., Pikuz, T.A., Romanova, V. & Shelkovenko, T.A. (1994). High-performance X-ray spectroscopic devices for plasma microsources investigations. *Physica Scripta* **50**, 333.

Gordon, H., Hobby, M.G. & Peacock, N.J. (1980). Classification of teh X-ray spectra of transitions in the Ne F and O I isoelectronic sequences of the elements from iron to bromine and in the Na I isoelectronic sequences of gallium to bromine. *J. Phys. B Atom. Molec. Phys.*. **13**, 1985–1999.

Hutcheon, R., Cooke, L., Key, M.H., Lewis, C.L. & Bromage, G.E. (1980). Neon-like and Fluorine-like X-ray emission spectra for elements from Cu to Sr. *Physica Scripta* **21**, 89–97.

Kelly, R.L. (1987). Atomic and ionic spectral lines below 2000 Å. *J. Phys. Chem. Ref. Data* **16**, 1.

Koenig, M., Boudenne, J.M., Legriel, P., Grandpierre, T., Batani, D., Bossi, S., Nicolella, S. & Benattar, R. (1997). A computer driven crystal spectrometer with CCD detectors for X-ray spectroscopy of laser-plasmas. *Review Scientific Instruments* **68**, 2387–2392.

Magunov, A., Faenov, A., Skobelev, I., Pikuz, T., Batani, D., Milani, M., Costato, M., Pozzi, A., Turcu, E., Allot, R., Koenig, M., Benuzzi, A., Flora, F. & Reale, A. (1998). Formation of the X-ray line emission spectrum of excimer laser-produced plasmas. *Laser Part. Beams,* **16**, 61–70.

Masini, A., Batani, D., Previdi, F., Costato, M., Pozzi, A., Turcu, E., Allott, R. & Lisi, N. (1999). Yeast cell metabolism investigated by C02 production and soft X-ray irradiation. *European Physics Journal: Applied Physics* **5**, 101–109.

Milani, M., Conte, A., Costato, M., Salsi, F., Baroni, G., Batani, D., Ferrario, L. & Turcu, E. (1999). NMR and pressure correlated analysis of metabolic changes in soft X-rays irradiated yeast cells. *European Physics Journal D* **5**, 267–270.

Pikuz, T.A., Faenov, A., Pikuz, S., Romanova, V.M., Shelkovenko, T.A. (1995). Bragg X-ray optics for imaging spectroscopy of plasma microsources. *J. X-Ray Sci. Technol.* **5**, 323.

Poletti, G., Orsini, F., Batani, D., Bernardinello, A., Desai, T., Ullschmied, J., Skala, J., Kralikova, B., Krousky, E., Pfeifer, M., Kadlec, Ch., Mocek, T., Präg, A., Renner, O., Cotelli, F., Lora Lamia, C. & Zullini, A. (2004). Soft X-ray Contact Microscopy of nematode *Caenorhabditis elegans*. *European Physical Journal D* **24**, 84–90.

Rockett, P.D., Bird, C.R., Hailey, C., Sullivan, D., Brown, D.B. & Burkalter, P.G. (1985). X-ray calibration of kodak DEF film. *Appl. Opt.* **24**, 2536.

Rosmej, F., Faenov, A., Pikuz, T., Flora, F., Di Lazzaro, P., Bollanti, S., Lisi, N., Letardi, T., Reale, A., Palladino, L., Batani, D., Bossi, S., Bernardinello, A., Scafati, A., Reale, L., Zigler, A., Fraenkel, M. & Cowan, E. (1997). Inner-shell satellite transitions in dense short pulse plasmas. *Journal Quant. Spectroscopy Radiation Transfer* **58**, 859–878.

Stepanov, A., Starostin, A., Roerich, V., Makhrov, V., Faenov, A., Magunov, A., Pikuz, T., Skobelelev, I., Flora, F., Bollanti, S., Di Lazzaro, P., Lisi, N., Letardi, T., Palladino, L., Reale, A., Batani, D., Bossi, S., Bernardinello, A., Scafati, A., Reale, L., Osterheld, A. & Goldstein, W. (1997). Modelling of the He-like magnesium spectral line radiation from the plasma created by XeCl and Nd-glass lasers. *Journal Quant. Spectroscopy Radiation Transfer* **58**, 937–952.

Turcu, E., Tallents, G.J., Ross, I., Michette, A.G., Schulz, M., Meldrum, R.A., Wharton, C.W., Batani, D., Martinetti, M. & Mauri, A. (1994*a*). Optimisation of an excimer laser-plasma soft X-ray source for applications in biophysics and medical physics. *Physica Medica* **10**, 93–99.

Turcu, E., Maldonado, J.R., Ross, I., Shields, H., Trenda, P., Batani, D., Fluck, P. & Goodson, H. (1994*b*). Calibration of an excimer laser-plasma source for X-ray lithography. *Microelectronic Engineering* **23**, 243–260.

Vergunova, G., Magunov, A., Dyakin, V., Faenov, A., Pikuz, T., Skobelev, I., Batani, D., Bossi, S., Bernardinello, A., Flora, F., Di Lazzaro, P., Bollanti, S., Lisi, N., Letardi, T., Reale, A., Palladino, P., Scafati, A., Reale, L., Osterheld, A. & Goldstein, W. (1997). Features of plasma produced by excimer laser at low intensities. *Physica Scripta* **55**, 483–490.